Proteins Hot Paper

DOI: 10.1002/anie.201308473

Single Mutations in Tau Modulate the Populations of Fibril Conformers through Seed Selection**

*Virginia Meyer, Paul D. Dinkel, Yin Luo, Xiang Yu, Guanghong Wei, Jie Zheng, Gareth R. Eaton, Buyong Ma, Ruth Nussinov, Sandra S. Eaton, and Martin Margittai**

Abstract: *Seeded conversion of tau monomers into fibrils is a central step in the progression of tau pathology in Alzheimer's disease and other neurodegenerative disorders. Self-assembly is mediated by the microtubule binding repeats in tau. There are either three or four repeats present depending on the protein isoform. Here, double electron-electron resonance spectroscopy was used to investigate the conformational ensemble of four-repeat tau fibrils. Single point mutations at key positions in the protein (ΔK280, P301S, P312I, D314I) markedly change the distribution of fibril conformers after template-assisted growth, whereas other mutations in the protein (I308M, S320F, G323I, G326I, Q336R) do not. These findings provide unprecedented insights into the seed selection of tau disease mutants and establish conformational compatibility as an important driving force in tau fibril propagation.*

Fibrils resulting from the aggregation of the microtubule-associated protein tau are the pathological hallmarks of numerous neurodegenerative disorders including Alzheimer's disease and frontotemporal dementia.[1,2] The propagation of tau fibrils is characterized by template-assisted conversion of monomers[3–5] and cell-to-cell transfer of aggregates[6] leading to prion-like spreading of protein aggregates in the brain.[7] Six different tau isoforms are expressed in the central nervous system, and can be grouped into three-repeat (3R) and four-repeat (4R) tau, based on the number of microtubule-binding repeats in the amyloidogenic core region.[1] An asymmetric barrier allows 4R tau to grow onto 3R tau seeds, but not vice versa.[8] Conformational differences between tau fibrils may play an important role in determining phenotypic diversity in human tauopathies.[9] In vitro experiments have demonstrated that fibrils of 4R tau are structurally heterogeneous and composed of at least three distinct conformers.[10] Structural heterogeneity is a common feature among amyloid fibrils and a potential basis for conformation-induced strain switching in prion propagation.[11,12] The investigation of heterogeneous amyloid ensembles, however, is challenging as multiple conformers have to be monitored at the same time.

To overcome this problem we have employed double electron-electron resonance (DEER) spectroscopy,[13] a technique which has been used to measure the distances between unpaired electrons of spin labels in proteins[14] and has emerged as a powerful new tool for elucidating fibril structure.[15] Importantly, DEER is capable of describing the relative populations of fibrils in a heterogeneous mixture.[10] Herein we report that single-point mutations in key positions of 4R tau affect seed selection and thereby alter the populations of fibril conformers. These findings establish conformational compatibility as an important determinant in fibril propagation.

To explore the seeding properties of tau, we used truncated versions of 4R tau (K18) and 3R tau (K19), which contain the repeat region that forms the structural core but not the disordered fuzzy coat.[16] These constructs show properties similar to their full-length counterparts with respect to cross-β structure,[17] strand registry,[18] seeding,[5] uptake,[19] and transmission,[20] yet have the advantage of greatly accelerated aggregation kinetics.[21] We selected a representative K18 double cysteine mutant, 311/328, with a heterogeneous conformation distribution[10] to examine differences in seed selection initiated by mutated monomers.

[*] V. Meyer, Dr. P. D. Dinkel, Prof. G. R. Eaton, Prof. S. S. Eaton, Prof. M. Margittai
Department of Chemistry and Biochemistry
University of Denver, Denver, CO 80208 (USA)
E-mail: martin.margittai@du.edu
Y. Luo, Prof. G. Wei
State Key Laboratory of Surface Physics, Key Laboratory for Computational Physical Sciences (MOE) and Department of Physics
Fudan University, Shanghai (P. R. China)
Dr. X. Yu, Prof. J. Zheng
Department of Chemical & Biomolecular Engineering
The University of Akron, Akron, OH 44325 (USA)
Dr. B. Ma, Prof. R. Nussinov
Leidos Biomedical Research, Inc.
Cancer and Inflammation Program
National Cancer Institute, Frederick National Laboratory
Frederick, MD 21702 (USA)
Prof. R. Nussinov
Sackler Institute of Molecular Medicine, Department of Human Genetics and Molecular Medicine, Sackler School of Medicine
Tel Aviv University, Tel Aviv 69978 (Israel)

[**] This project was supported by the National Institute of Neurological Disorders and Stroke Grant R01NS076619 (to M.M.). This work was also supported by the National Cancer Institute Contract (HHSN261200800001E), the intramural research program of the National Cancer Institute Center for Cancer Research, National Science Foundation (CAREER Award CBET-0952624 and CBET-1158447; to J.Z.), and the National Natural Science Foundation of China Grant (11074047, 11274075, and 91227102; to G.W.). We thank Dr. Eric Hustedt for his assistance using GLADD, and helpful discussions regarding analysis of DEER data.

Supporting information for this article is available on the WWW under http://dx.doi.org/10.1002/anie.201308473.

The following mutations were incorporated into the K18 311/328 core: known disease-related mutants of ΔK280,[22] P301S,[23] S320F,[24] Q336R,[25] and additional mutants of I308M, P312I, D314I, G323I, G326I. The latter mutants are not found in humans, but were chosen based on their potential effects on seed selection because of the position in the protein and the nature of the amino acid change. All mutated monomers grew onto the templates provided by K18 wild-type (WT) seeds. Interactions between spin labels of stacked tau molecules were avoided by diluting samples with a 50-fold molar excess of K18 WT. Resultant DEER data were analyzed analogously for all samples to detect whether the mutants grew preferentially onto specific fibril conformations present in the mixture. Variations in seed selection were determined through comparison to the distance distribution of the nonmutated K18 311/328.

Before analysis of mutation effects, it was important to demonstrate that the K18 311/328 system is robust for use as an indicator of conformational variation. The sample was prepared and analyzed in triplicate and the distribution shown to be reproducible (Figure 1a). When prepared with different seed batches, we consistently observed three distances for this system at 3.2, 3.8, and 4.8 nm. The relative populations of fibrils adopting these conformations are also well-conserved (for data analysis, see Experimental Procedures and Figures S1 and S2 in the Supporting Information). We therefore concluded that K18 311/328 was an appropriate starting point for examining variations in conformation selection of mutated monomer grown onto K18 WT seeds.

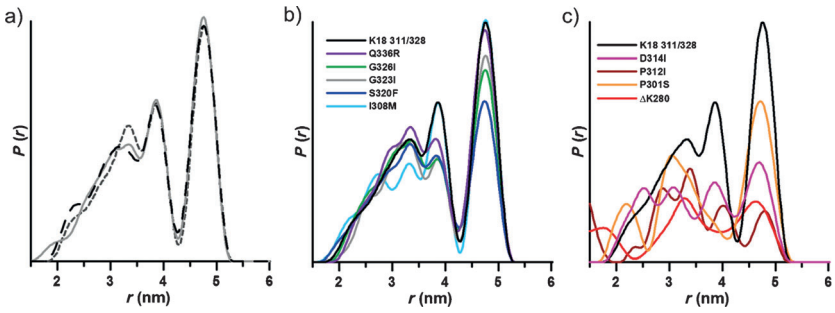

Figure 1. Distance distributions of K18 311/328: a) reproducibility, b) mutants with distance distributions similar to nonmutated K18 311/328, c) mutants with very different distributions compared to nonmutated K18 311/328.

We next examined the distance distributions for the mutant-bearing fibrils and found that several of the mutations gave distributions similar to that of the nonmutated K18 311/328 (Figure 1b). Conversely, some of the mutations at significant positions in the protein (ΔK280, P301S, P312I, and D314I) clearly changed the distribution of fibril conformers generated by template-assisted growth (Figure 1c). The spin-labeled proteins did not affect overall aggregation kinetics (see Figure S3). The addition of ΔK280 to K18 311/328 also did not alter the underlying distance distribution (see Figure S4). These data suggest that individual mutants do not confer their growth properties onto K18 WT or K18 311/328, but instead act independently.

It is noteworthy that the labeling efficiencies for all tau mutants were similar (see Figure S5), thus excluding the possibility that incomplete labeling of tau monomers resulted in the different peak patterns observed in Figure 1c. To ensure that the dramatic changes in seed selection were not a result of amorphous monomer aggregation, fibril formation was confirmed by electron microscopy (EM) (see Figure S6). Furthermore, continuous wave electron paramagnetic resonance measurements verified that the mutant monomers became incorporated into the fibrils (see Figure S7). The spectra revealed no major broadening, thus indicating the absence of large subpopulations with spin labels less than 2 nm apart. Spin labels separated by more than 5 nm are out of the detectable range for the DEER measurements presented herein.[10]

We propose that key mutations play a role in seed selection during fibril growth, whereas mutations with similar distributions have little or no conformational effect. In addition to variation in distance distributions, examination of the DEER data supports these conclusions. When grouped according to degree of similarity to nonmutated K18 311/328, the traces and fit functions for the background-subtracted data align with the grouping of similar and dissimilar distance distributions (see Figures S8–S10). The initial drop in signal of the raw data before background subtraction provides a qualitative measure of the interaction between the spin labels. In this area of the data, similar mutants trace together and different mutants trace separately, with the ΔK280 mutant being the furthest outlier (Figure 2).

A shallow initial drop in the raw data corresponds to weak spin–spin interactions. These data suggest that the mutations with very different population distributions may contain conformers with interspin distances

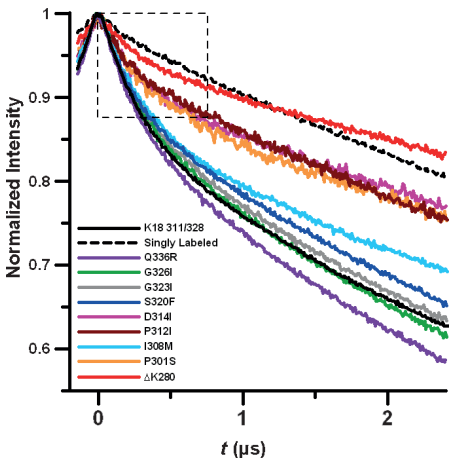

Figure 2. Overlay of raw DEER data for all mutants studied, including the K18 311/328 core and singly labeled monomer (all data are normalized to the maximum signal intensity = 1). The largest difference is apparent from the initial drop region as indicated by the dotted box.

larger than 5 nm. This quality was previously shown for K19 fibrils[10] and now for ΔK280. Note that the ΔK280 mutation resides in the second microtubule binding repeat and hence only occurs in 4R tau. Adoption of extended-monomer conformations may account for the asymmetric seeding barrier demonstrated for tau,[8] for which K18 can grow onto K19 fibrils, but K19 cannot grow onto K18. Since K18 ΔK280 may also adopt a more extended conformation, it was logical to test whether K19 could be grown onto pure K18 ΔK280 seeds. To determine whether K18 ΔK280 seeds can recruit K19 we utilized an intrinsic acrylodan assay[8] to assess K19 aggregation. Acrylodan-labeled K19 tau without the introduction of K18 ΔK280 seeds produced a fluorescence spectrum with a λ_{max} of around 522 nm, typical of monomeric tau. When K18 ΔK280 seeds were added to K19 and incubated for 2 hours, the λ_{max} of labeled K19 tau significantly blue-shifted, thus indicating the growth of K19 on K18 ΔK280 seeds (Figure 3a). For kinetic traces and comparison with

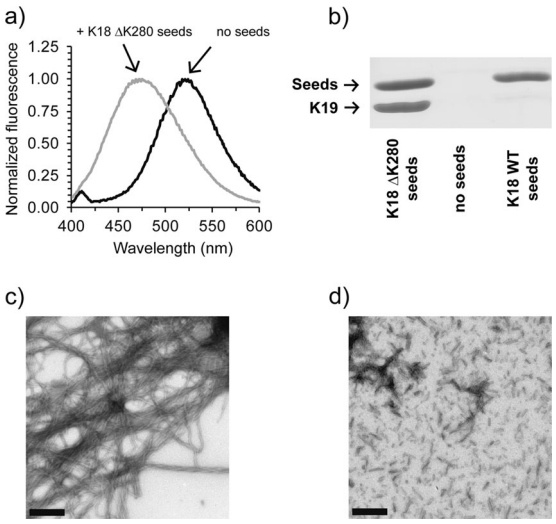

Figure 3. K19 grows on K18 ΔK280 seeds. a) Fibril formation is monitored by acrylodan fluorescence and is accompanied by a blue shift from $\lambda = 522$ to 478 nm. b) Sedimentation confirms K19 growth onto K18 ΔK280 but not K18 WT (quantitation in Figure S4). c) EM images of K19 WT (10 μM) grown onto 10% K18 ΔK280 seeds after 3 h of incubation at 37 °C, and d) of ΔK280 seeds without K19 WT addition. Bar = 400 nm.

K18- and K19-seeded reactions see Figure S11. To independently confirm K19 growth on K18 ΔK280 seeds, we carried out sedimentation experiments of seeded reactions. In contrast with K18 WT seeds, K18 ΔK280 seeds were shown to effectively seed the K19 monomer (Figure 3b, see Figure S12 in the Supporting Information for triplicate quantification). Importantly, the ability of K18 ΔK280 to seed K19 is not due to K18 ΔK280 fibrils aggregating more efficiently, as the sedimented seeds of K18 WT and K18 ΔK280 seeds were found to be of comparable density. Growth of K19 on K18 ΔK280 seeds is furthermore supported by EM images taken after a K18 ΔK280 seeded reaction, thus revealing an abundance of long fibrils which can be clearly distinguished from the short and fragmented K18 ΔK280 seeds (Figure 3c and d). The new seeding competency of K18 ΔK280 is in line with this protein having a different conformation from K18 WT[3] and emphasizes how a single-point mutation can effectively change the functional properties of a fibril.

In conclusion, DEER spectroscopy has provided a unique tool to study variations in protein conformation. We utilized this tool to investigate the effects of single-point mutations on seed selection. We observe that some mutants of tau, when grown onto WT seeds, retain the composition of the original ensemble, while other mutants significantly alter the populations of conformers (schematically summarized in Figure 4).

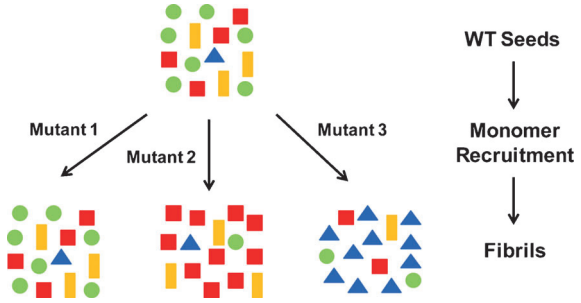

Figure 4. General model for sequence-dependent seed selection in tau fibril growth. Tau mutants that are fully compatible with the conformational ensemble of WT tau seeds retain the original composition of conformers (Mutant 1). Mutants that are not compatible cause a switch in the dominant species (Mutant 2) and in some cases may amplify a minor subspecies (Mutant 3). The reverse process in which monomers of WT tau grow onto mutant seeds will follow similar selection rules based on conformational compatibility. Symbols with different color and shape represent different conformers of tau fibrils.

These effects can be explained by the conformational compatibilities of individual mutants. Mutants that do not interfere with any of the original conformers will be recruited akin to the WT monomer. Mutants that are incompatible with some of the original conformers will change the overall composition of the ensemble. While these selection processes could undoubtedly be modulated by additional factors in the complex cellular environment of the human brain, our findings provide an important general model of how new fibril ensembles might emerge. It is plausible that the conformational composition of tau fibrils could vary for different forms of inherited frontotemporal dementia, where dominant mutations in the tau gene (*MAPT*) are linked to disease. Also important in the context of the herein presented study, it seems that in at least some cases somatic mutations in tau could define the initial ensemble of conformers in sporadic forms of tauopathies and hence influence the selective processes as fibrils spread throughout the brain. Specifically, if different fibril ensembles composed of mutant tau were transferred to connected neurons (free of tau mutations) the recruitment of WT tau would vary in a conformation-dependent manner. The presented model shows striking similarities to current models of strain mutation and selection in prions.[11] Remarkably, a single amino acid difference at position 226 in the prion proteins of elk and deer, combined with conformational selection of compatible

seeds, determines strain mutation in chronic wasting disease.[26] Although transmissibility of tau is confined to neurons within a single human brain, the overall conformational selection processes appear to be governed by the same underlying structural principles. It is likely that other pathological amyloid fibrils share similar selection properties. The recent finding that structural variations in fibrils of the β-amyloid peptide may contribute to variations in Alzheimer's disease[27] underscores the biological relevance of fibril conformation. Changes in fibril conformation through seed selection could be an important molecular mechanism of diversifying disease phenotype. The existence of different fibril ensembles and their emergence upon spreading must be taken into account when designing new therapeutic strategies for interfering with amyloid diseases.

Received: September 28, 2013
Revised: November 13, 2013
Published online: January 22, 2014

Keywords: Alzheimer's disease · conformation analysis · EPR spectroscopy · proteins · tau fibrils

[1] M. G. Spillantini, M. Goedert, *Lancet Neurol.* **2013**, *12*, 609 – 622.
[2] V. M. Lee, M. Goedert, J. Q. Trojanowski, *Annu. Rev. Neurosci.* **2001**, *24*, 1121 – 1159.
[3] B. Frost, J. Ollesch, H. Wille, M. I. Diamond, *J. Biol. Chem.* **2009**, *284*, 3546 – 3551.
[4] T. Nonaka, S. T. Watanabe, T. Iwatsubo, M. Hasegawa, *J. Biol. Chem.* **2010**, *285*, 34885 – 34898.
[5] J. L. Guo, V. M. Lee, *J. Biol. Chem.* **2011**, *286*, 15317 – 15331.
[6] a) N. Kfoury, B. B. Holmes, H. Jiang, D. M. Holtzman, M. I. Diamond, *J. Biol. Chem.* **2012**, *287*, 19440 – 19451; b) B. Frost, R. L. Jacks, M. I. Diamond, *J. Biol. Chem.* **2009**, *284*, 12845 – 12852; c) A. de Calignon, M. Polydoro, M. Suarez-Calvet, C. William, D. H. Adamowicz, K. J. Kopeikina, R. Pitstick, N. Sahara, K. H. Ashe, G. A. Carlson, T. L. Spires-Jones, B. T. Hyman, *Neuron* **2012**, *73*, 685 – 697; d) L. Liu, V. Drouet, J. W. Wu, M. P. Witter, S. A. Small, C. Clelland, K. Duff, *PLoS One* **2012**, *7*, e31302.
[7] a) H. Braak, K. Del Tredici, *Acta Neuropathol.* **2011**, *121*, 589 – 595; b) M. Goedert, F. Clavaguera, M. Tolnay, *Trends Neurosci.* **2010**, *33*, 317 – 325; c) A. Aguzzi, L. Rajendran, *Neuron* **2009**, *64*, 783 – 790; d) P. Brundin, R. Melki, R. Kopito, *Nat. Rev. Mol. Cell Biol.* **2010**, *11*, 301 – 307; e) B. Frost, M. I. Diamond, *Nat. Rev. Neurosci.* **2010**, *11*, 155 – 159; f) M. Jucker, L. C. Walker, *Nature* **2013**, *501*, 45 – 51.
[8] P. D. Dinkel, A. Siddiqua, H. Huynh, M. Shah, M. Margittai, *Biochemistry* **2011**, *50*, 4330 – 4336.
[9] F. Clavaguera, H. Akatsu, G. Fraser, R. A. Crowther, S. Frank, J. Hench, A. Probst, D. T. Winkler, J. Reichwald, M. Staufenbiel, B. Ghetti, M. Goedert, M. Tolnay, *Proc. Natl. Acad. Sci. USA* **2013**, *110*, 9535 – 9540.
[10] A. Siddiqua, Y. Luo, V. Meyer, M. A. Swanson, X. Yu, G. Wei, J. Zheng, G. R. Eaton, B. Ma, R. Nussinov, S. S. Eaton, M. Margittai, *J. Am. Chem. Soc.* **2012**, *134*, 10271 – 10278.
[11] J. Collinge, A. R. Clarke, *Science* **2007**, *318*, 930 – 936.
[12] a) J. Li, S. Browning, S. P. Mahal, A. M. Oelschlegel, C. Weissmann, *Science* **2010**, *327*, 869 – 872; b) D. A. Bateman, R. B. Wickner, *PLoS Genet.* **2013**, *9*, e1003257.
[13] a) A. D. Milov, K. M. Salikhov, M. D. Shchirov, *Sov. Phys. Solid State* **1981**, *23*, 565 – 569; b) G. Jeschke, M. Pannier, H. W. Spiess, *Biol. Magn. Reson.* **2000**, *19*, 493 – 512.
[14] G. Jeschke, *Annu. Rev. Phys. Chem.* **2012**, *63*, 419 – 446.
[15] a) I. Karyagina, S. Becker, K. Giller, D. Riedel, T. M. Jovin, C. Griesinger, M. Bennati, *Biophys. J.* **2011**, *101*, L1 – 3; b) S. Bedrood, Y. Li, J. M. Isas, B. G. Hegde, U. Baxa, I. S. Haworth, R. Langen, *J. Biol. Chem.* **2012**, *287*, 5235 – 5241; c) S. Pornsuwan, K. Giller, D. Riedel, S. Becker, C. Griesinger, M. Bennati, *Angew. Chem.* **2013**, *125*, 10480 – 10484; *Angew. Chem. Int. Ed.* **2013**, *52*, 10290 – 10294.
[16] a) C. M. Wischik, M. Novak, H. C. Thogersen, P. C. Edwards, M. J. Runswick, R. Jakes, J. E. Walker, C. Milstein, M. Roth, A. Klug, *Proc. Natl. Acad. Sci. USA* **1988**, *85*, 4506 – 4510; b) S. Wegmann, I. D. Medalsy, E. Mandelkow, D. J. Muller, *Proc. Natl. Acad. Sci. USA* **2013**, *110*, E313 – 321.
[17] a) M. von Bergen, S. Barghorn, L. Li, A. Marx, J. Biernat, E. M. Mandelkow, E. Mandelkow, *J. Biol. Chem.* **2001**, *276*, 48165 – 48174; b) J. Berriman, L. C. Serpell, K. A. Oberg, A. L. Fink, M. Goedert, R. A. Crowther, *Proc. Natl. Acad. Sci. USA* **2003**, *100*, 9034 – 9038.
[18] a) M. Margittai, R. Langen, *Proc. Natl. Acad. Sci. USA* **2004**, *101*, 10278 – 10283; b) A. Siddiqua, M. Margittai, *J. Biol. Chem.* **2010**, *285*, 37920 – 37926.
[19] B. B. Holmes, S. L. Devos, N. Kfoury, M. Li, R. Jacks, K. Yanamandra, M. O. Ouidja, F. M. Brodsky, J. Marasa, D. P. Bagchi, P. T. Kotzbauer, T. M. Miller, D. Papy-Garcia, M. I. Diamond, *Proc. Natl. Acad. Sci. USA* **2013**, *110*, E3138 – 3147.
[20] M. Iba, J. L. Guo, J. D. McBride, B. Zhang, J. Q. Trojanowski, V. M. Lee, *J. Neurosci.* **2013**, *33*, 1024 – 1037.
[21] S. Barghorn, E. Mandelkow, *Biochemistry* **2002**, *41*, 14885 – 14896.
[22] P. Rizzu, J. C. Van Swieten, M. Joosse, M. Hasegawa, M. Stevens, A. Tibben, M. F. Niermeijer, M. Hillebrand, R. Ravid, B. A. Oostra, M. Goedert, C. M. van Duijn, P. Heutink, *Am. J. Hum. Genet.* **1999**, *64*, 414 – 421.
[23] O. Bugiani, J. R. Murrell, G. Giaccone, M. Hasegawa, G. Ghigo, M. Tabaton, M. Morbin, A. Primavera, F. Carella, C. Solaro, M. Grisoli, M. Savoiardo, M. G. Spillantini, F. Tagliavini, M. Goedert, B. Ghetti, *J. Neuropathol. Exp. Neurol.* **1999**, *58*, 667 – 677.
[24] S. M. Rosso, E. van Herpen, W. Deelen, W. Kamphorst, L. A. Severijnen, R. Willemsen, R. Ravid, M. F. Niermeijer, D. Dooijes, M. J. Smith, M. Goedert, P. Heutink, J. C. van Swieten, *Ann. Neurol.* **2002**, *51*, 373 – 376.
[25] S. M. Pickering-Brown, M. Baker, T. Nonaka, K. Ikeda, S. Sharma, J. Mackenzie, S. A. Simpson, J. W. Moore, J. S. Snowden, R. de Silva, T. Revesz, M. Hasegawa, M. Hutton, D. M. Mann, *Brain* **2004**, *127*, 1415 – 1426.
[26] R. C. Angers, H. E. Kang, D. Napier, S. Browning, T. Seward, C. Mathiason, A. Balachandran, D. McKenzie, J. Castilla, C. Soto, J. Jewell, C. Graham, E. A. Hoover, G. C. Telling, *Science* **2010**, *328*, 1154 – 1158.
[27] J. X. Lu, W. Qiang, W. M. Yau, C. D. Schwieters, S. C. Meredith, R. Tycko, *Cell* **2013**, *154*, 1257 – 1268.

